Estimating ammonia emissions from cropland in China based on the establishment of agro-region-specific models

Hua Wu,[†] Yunpeng Li,[†] Zihao Xie,[†] Jianfei Sun,[†] Pete Smith,[‡] Kun Cheng,[*,†] Pinhao Fan,[†] Qian Yue,[§] Genxing Pan[†]

[†] Institute of Resource, Ecosystem and Environment of Agriculture, and Jiangsu Collaborative Innovation Center for Solid Organic Waste Resource Utilization, Nanjing Agricultural University, 1 Weigang, Nanjing, Jiangsu 210095, China

[‡] Institute of Biological and Environmental Sciences, School of Biological Sciences, University of Aberdeen, Aberdeen AB24 3UU, U.K.

[§] Key Laboratory for Crop and Animal Integrated Farming of Ministry of Agriculture and Rural Affairs/Recycling Agriculture Research Center, Jiangsu Academy of Agricultural Sciences, Nanjing 210014, China

Corresponding Author

*E-mail: chengkun@njau.edu.cn Tel.: +86 25 8439 9852 Fax: +86 25 8439 9852

Running head: Ammonia emissions in China's cropland

Abstract: Estimating ammonia (NH_3) volatilization from cropland can identify potential environmental risks and is also important for mitigating NH_3 loss, since cropland is the major anthropogenic source of NH_3. Reducing uncertainties around NH_3 volatilization estimates is a key need. In this study, both a single national model and agro-region-specific models were developed to embody the variation of NH_3 volatilization associated with environmental attributes and management practices for cropland in various agro-regions of China. A database with 951 field measurements across China was established to develop and evaluate the model, in which 75% of the measurements were used for model fitting and 25% were used for evaluation. The agro-region specific model had a better performance than the single national scale model, and the agro-region-specific model could successfully simulate NH_3 emissions with R^2 values of 0.41–0.93 as a function of crop type, N fertilizer type and rate, timing of fertilization, soil pH, clay content, bulk density, precipitation, air temperature, and soil total nitrogen content. Inputting high-resolution spatial data into the model, the NH_3 emissions from China's cropland were estimated to be 4.31 Tg NH_3-N in the year 2015 with a 95% confidence interval of 3.64–5.64 Tg NH_3-N, of which paddy rice cultivation accounted for 44%, and maize and wheat cultivation contributed 20% and 16%, respectively. Notable spatial variability was also found in NH_3 emissions from China’s cropland due to regional differences in climate, soil and management patterns. This study showed that the accuracy of estimation of farmland NH_3 emissions can be improved by taking meteorological, soil and management variables into account and inputting high-spatial-resolution data into the modeling.

Key words: NH_3; crop; regression model; spatial variability; N fertilizer

1 Introduction

Ammonia (NH_3) emissions have direct and indirect impacts on human health and ecosystem quality. NH_3 is often converted to ammonium nitrogen (NH_4^+-N) under acidic conditions, while NH_4^+-N returned to the ecosystem through wet deposition leads to eutrophication of rivers and lakes, and causes soil acidification and further threatens ecosystem health (Krupa, 2003; Bouwman, 1999; Anderson et al., 2003). NH_3 is also an important precursor for the formation of atmospheric aerosol fine particles $PM_{2.5}$ (Battye et al., 2003). Agriculture is recognized as a main source of atmospheric NH_3, contributing 90% of global anthropogenic NH_3 emissions, of which N fertilization accounted for 40% of agricultural emissions (Galloway et al., 2004; Gao et al., 2013). At present, the annual global consumption of synthetic N fertilizer is up to 100.8 million tonnes (Mt), which resulted in 16.7 Tg N of NH_3 volatilization in 2010 (FAO, 2018; Xu et al., 2019). The environmental risks of NH_3 emissions are also likely to increase, so effective management of NH_3 volatilization is imperative. Given these facts, there is an urgent need for a high-precision and high-resolution NH_3 emission inventory, where the premise of an emission inventory is to develop a reliable method with low uncertainty.

Methods to estimate NH_3 volatilization generally include a volatility factor and a model method. In view of the fact that only one input variable, N input, is required, globally constant or region-specific volatility factors have often been used to estimate NH_3 emissions at global or national scale where data were limited (Streets et al., 2003; Riddick et al., 2016). The Intergovernmental Panel on Climate Change (IPCC) proposed a NH_3 emission factor of 14.2% due to urea application; however, using the IPCC volatility factor to estimate regional NH_3 emissions can result in great uncertainty (IPCC, 2019). To address this issue, more specific volatility factors that account for fertilizer types and other climatic / environmental factors have been developed in some studies (Bouwman et al., 1997; Yan et al., 2003; Huang et al., 2012; Xu et al., 2015). Xu et al. (2019) compared global estimates of NH_3 volatilization estimated by the IPCC volatility factor and process-based model DLEM-Bi-NH_3 and found that the IPCC volatility factor (10%) estimates were half those estimated by DLEM-Bi-NH_3, suggesting a big difference between the volatility factor methods. It has been well recognized that climate, soil and management factors can have a significant impact on NH_3 volatilization, and some models, considering complex ecological processes, have been developed to simulate NH_3 emissions (Zhang et al., 2011;

Wu et al., 2017). For example, the DLEM-Bi-NH_3 module was developed from the process-based Dynamic Land Ecosystem Model (DLEM) ecosystem model to simulate NH_3 volatilization process regulated by environmental factors and plant growth, and this module can simulate NH_3 volatilization under various conditions at a daily time step (Tian et al., 2015; Xu et al., 2018). Based on a Bayesian Recursive Regression Tree algorithm, a nonlinear NH_3 volatilization model by Zhou et al. (2016) also performed well in China's cropland. Process-based or nonlinear models could estimate NH_3 emissions with low uncertainty, but these models require very detailed input data, which may limit the application in areas where data is lacking. A relatively simple regression model, that requires easy-to-access input data, could help to overcome the data requirement issues faced by process models, but such studies are limited.

China's total annual grain production increased by 93% from 1980 to 2015, while N fertilizer use increased by 3 times from 9.34 Mt yr^{-1} to 23.62 Mt yr^{-1} during this period (DRSES-SBS, 2016). According to the law of diminishing returns of N fertilizer on yield, the substantial increase in N fertilizer input did not significantly increase crop yields, resulting in low nitrogen use efficiency (27.5%-38%) and loss of reactive N into the environment (Zhang et al., 2007; Yan et al., 2014). As estimated by Xu et al. (2018), NH_3 volatilization increased from 2.8 Tg NH_3-N in 1990 to 4.3 Tg NH_3-N in 2010. A high-resolution NH_3 emission inventory is necessary for policy makers to develop the regionally specific mitigation strategies. There have been previous studies estimating NH_3 emissions in China's cropland using different methods, but the variation in the estimates between different studies is large. For example, Fu et al. (2015) estimated that emissions in 2011 were 3 Tg NH_3-N, which is very different from the emissions of 4.3–4.5 Tg NH_3-N in 2010 estimated by Xu et al. (2015) and Xu et al. (2018), although the application rate of N fertilizer in 2011 was higher than that in 2010, and Fu et al. (2015) considered more crops than Xu et al. (2018). Moreover, few studies conducted uncertainty analysis in estimations, and the uncertainty ranged from 19% to greater than 50% (Streets et al., 2003; Zhou et al., 2016; Zhang et al., 2011; Huang et al., 2012). Previous studies mainly focused on a single model or volatile factors at the national scale; however, China has nine first-level terrestrial agro-regions with high spatial heterogeneity of climatic conditions, soil properties, and management patterns (NARC, 1991). We hypothesized that the development of agro-region-specific model would improve the simulation accuracy of NH_3 emissions in croplands.

In order to achieve broad applicability and reduce uncertainty, there is an urgent need to develop an empirical regression model that can be driven with limited variables. The objective of this study is to establish a single national and agro-region-based regression models of NH_3 volatilization and compare models performance based on a database of 964 observations. Using the developed model, the spatial distribution of NH_3 emissions was described, and NH_3 emissions of different crops were compared. Finally, an estimate of total NH_3 emissions from crop cultivation in China was made and the uncertainty of the model was quantified.

2 Materials and methods

2.1 Data sources

Data on seasonal NH_3 volatilization and climate/environment/management variables were collected for model development. A literature search of the China National Knowledge Infrastructure (CNKI) and Web of Science was conducted, with “ammonia”, “NH_3”, “reactive nitrogen”, “emission”, “fertilizer”, and “China” as the search keywords. We considered only data from original studies with direct NH_3 volatilization monitoring in the field, and data from incubations or simulations were excluded. NH_3 emission data during the crop growing season (defined as a period from planting to harvest for a given crop) at the experimental sites were collected. A dataset of 138 studies with a total of 951 seasonal cumulative NH_3 emission measurements over a time span of 1997-2018 was compiled, including 601 observations from upland crop cultivation and 350 observations from paddy rice cultivation (Fig. 1). The sites are located between the longitude of 86° to 126.7° and latitude of 19.5° to 45.5°. The dataset included the following information: seasonal cumulative NH_3 emissions; geographic information; weather data including annual mean temperature and annual precipitation; soil characteristics including soil organic carbon content, soil total nitrogen content, clay content, bulk density and pH; cropping rotation system; crop growing season data including planting date, transplanting date, and harvest date; crop types aggregated into 6 broad categories: rice, wheat, maize, vegetable, legume and others; fertilizer types classified into 5 broad categories; fertilizer application rate; fertilization times ; management practices including tillage type, straw return, and irrigation (Table 1).

According to the characteristics of natural conditions (climate, soil, water, biology, natural disasters, etc.) and socio-economic conditions (labor, technical equipment, transportation conditions, regional economic development level, etc.), China is divided into ten first-level agro-regions, including nine terrestrial agro-regions and one marine aquatic region (Table 1; NARC, 1991). Due to limitations of data availability in some agro-regions, the nine land agro-regions were aggregated into six including Northeast (NE), Loess Plateau & Inner Mongolia and along the Great Wall (LPIM), Gansu-Xinjiang & Qinghai-Tibet (GXQT), Huang-Huai-Hai (HHH), Yangtze River (YR), South & Southwest (SSW) in this study. Detailed information about the dataset can be found in Table S1.

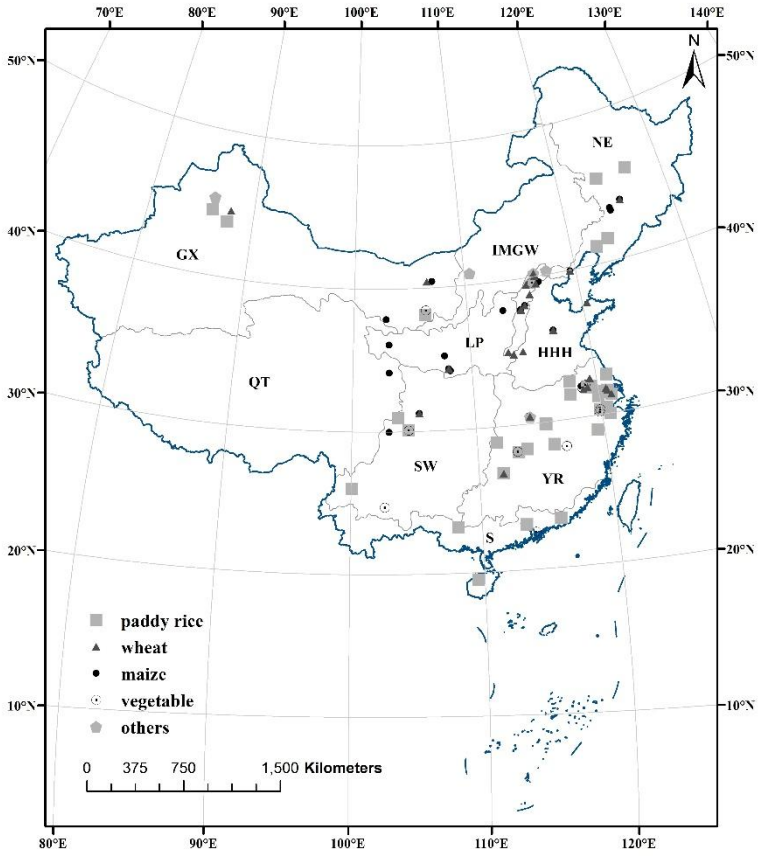

Fig. 1 Geographical distribution of experimental sites in China that were used for establishment of the NH_3 emission model

Table 1 Reclassified parameters used in model establishment

(a) fertilizer types	**Acronym**
Control without fertilizer application	Control
Mineral fertilizer	Min
Mineral fertilizer and organic material	Min & Org
Organic material	Org
Control release fertilizer, nitrification inhibitors, urease inhibitors	CI
(b) Agricultural areas	**Acronym**
Northeast	NE
Inner Mongolia and along the Great Wall	IM
Huang-Huai-Hai	HHH
Loess Plateau	LP
Yangtze River	YR
Southwest	SW
South	S
Gansu-Xinjiang	GX
Qinghai-Tibet	QT

2.2 Model development and evaluation

Measurements were randomly split into two groups for each agro-region using the R command "sample": 75% on average for model development and 25% on average held back for model evaluation. To meet the assumption for performing a regression analysis, the normality of the cumulative NH_3 emissions data were first tested before fitting the model, and were found not conform to the normal distribution, so the original data of cumulative NH_3 emissions were subjected to natural logarithmic transformation (Zuur et al., 2007). We also detected the correlation between variables to avoid collinearity among explanatory variables in the model.

The effects of all factors on the natural logarithmic transformed dependent variable, ln (Cumulative NH_3 emission), was investigated by fitting a multiple regression model. The steps for performing model selection using stepwise regression were as follows: the threshold of significance was set to $p<0.05$, so variables with $p>0.05$ were discarded first; then a set of linear regression models, including different combinations of potential explanatory variables, was fitted; finally, the optimal model was selected based on the Akaike information criterion (AIC) and coefficient of determination (R^2) (Table S2). The formula of the model is as follows:

$$\ln(y) = \alpha + \sum_{i}^{N} \beta_i x + \varepsilon$$

Where y is the target dependent variable, Cumulative NH_3 emissions, in kg N ha^{-1} day^{-1}, and x represents the potential explanatory variables. While α and β_i represent the model coefficients, ε is the model error. All model regressions were constructed using the r command "lm". Both a single model of the entire Chinese cropland and six regional models were fitted to determine which model worked best. The relative contributions of each variable in the model was elucidated by conducting variance analysis.

We adopted the model evaluation framework proposed by Smith et al. (1997) to evaluate the six agro-region specific models developed. First, correlation analysis of simulated and measured NH_3 emissions was performed to assess whether simulated values follow the same pattern as measured values, and an R-squared value was calculated to assess the strength of the correlation. Then, relative root mean square error (rRMSE), modelling efficiency (*ME*) and mean difference (*E*) were calculated to evaluate the model performance. The t statistic was also calculated to test the significant difference between the simulated and measured values.

2.3 Simulation of NH_3 emissions from crop cultivation in China

In order to conduct the spatial analysis, spatial data of the variables were collected in this study. Climate data were obtained from the China Meteorological Data Web (http://data.cma.cn/), and soil data were obtained from the Harmonized World Soil Database at a spatial resolution of 5×5 min (FAO/IIASA/ISRIC/ISS-CAS/JRC, 2012). The planting area of each crop in 2015 was obtained from Monfreda et al. (2008) and data for N fertilizer application rates were obtained from Mueller et al. (2012) and the China Agricultural Cost-Benefit Data Assembly (DP-NDRC, 2016). The sum of crop area and fertilizer application amounts in all the grid cells of each province was matched to the statistics of the same province in 2015. The resolution of all spatial data was unified to 5×5 min.

The developed agro-region-specific models were projected onto a grid map of the agro-regions, and the seasonal NH_3 emissions per unit area of various crops were then simulated using the spatial data of variables used in the model. The total NH_3 emission in each grid were calculated by multiplying the NH_3 emissions per unit area by the corresponding crop area in each grid. We sorted all crops into 6 major groups including grain crops (paddy rice, wheat, maize, barley, millet, sorghum), legumes (soybean), oil-bearing crops (groundnut, rapeseed, and sunflower), vegetables (vegetables, potato), fruit (apple, citrus), and industrial crops (cotton, tobacco, sugarcane, beetroot). The seasonal emissions of each crop and each group of crops were simulated and calculated.

The uncertainty of the simulated NH_3 emissions was determined by calculating the 95% confidence interval (CI) (Chambers et al., 1993). National NH_3 emissions in cropland were the sum of NH_3 emissions of various crops, and the uncertainty of the total inventory was quantified using a quantitative method for combining uncertainties proposed by IPCC (2000).

All calculations and data processing were conducted in R (version 3.4.0), and the maps were generated by ArcGIS 10.2.

3 Results

3.1 NH_3 volatilization model establishment

Using the stepwise regression method, a national-scale model and six agro-region-specific models were established (Table 2; Table S3). By contrast, the R^2 of the agro-region-specific models ranged from 0.41 to 0.93, most of which were higher than that of the single model. The significant variables for the national-scale model were N fertilization rate, fertilizer type, fertilization times, soil pH, soil total N, crop type, annual precipitation. The structure of the six agro-region-specific models exhibited spatial differences. The N fertilization rate, fertilizer type, and crop type remained as variables in all models, explaining 10%–46%, 1%–5%, and 2%–12% of the variation, respectively. Fertilization times, contributing 2% to 24% to the variation, remained in five models except the NE model. Climate variables remained in the models of LPIM, GXQT, YR and SSW. Soil pH remained in the models of GXQT (50%), HHH (11%) and YR (6%), while soil total N content remained in the models of LPIM (47%), YR (9%) and HHH (1%). Soil physical properties including clay content and bulk density remained as variables in the models of LPIM, SSW and NE, HHH regions (Table 2; Fig. 2).

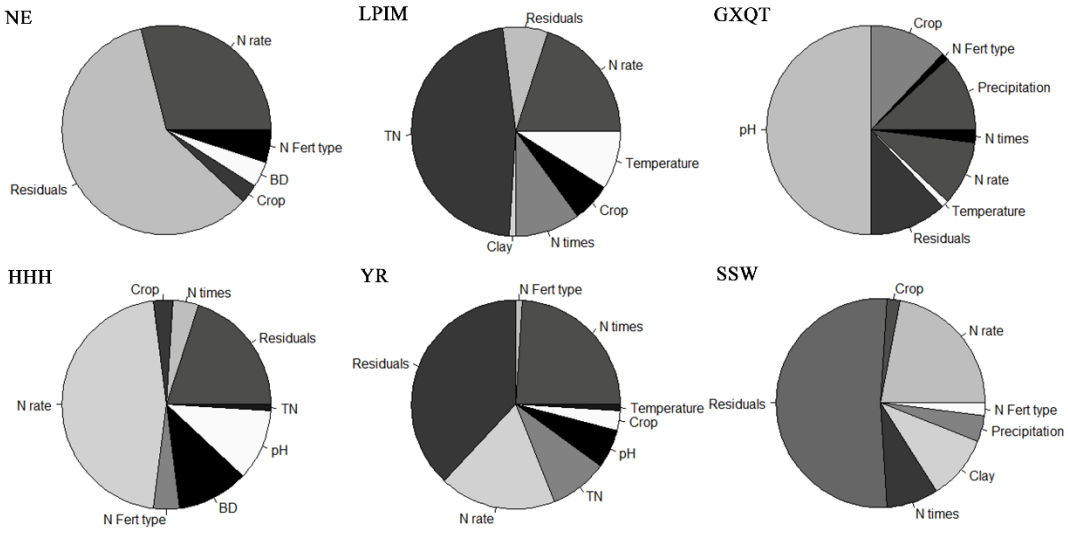

Fig. 2 Contributions of each variable to the NH_3 volatilization models

Table 2 NH_3 volatilization models of six agro-regions

Regions	Model	Coefficient$_1$ and Coefficient$_2$	R^2
NE (n=133)	$\ln(Cum\ NH_3) = -2.864 + 0.008N\ rate + 3.08BD + Coefficient_1 + Coefficient_2 + \varepsilon$	Others:0; Rice:0.482; CI:0; Min:-0.0021; Org:-0.0066; MinOrg:-0.0046	0.41
LPIM (n=52)	$\ln(Cum\ NH_3) = -13.68 + 0.006N_{rate} + 4.552soil\ total\ N + 1.43Temp - 0.088Clay + 0.168N\_times + Coefficient_1 + \varepsilon$	Maize:0; Wheat:0.631; Others:0.735	0.93
GXQT (n=63)	$\ln(Cum\ NH_3) = -59.39 + 0.002N\ rate + 6.221pH + 1.481Temp - 0.0096Prec + 0.289N\_times + Coefficient_1 + Coefficient_2 + \varepsilon$	Others:0; Rice:-1.614 MinOrg:0; Min:0.0057	0.88
HHH (n=102)	$\ln(Cum\ NH_3) = 6.596 + 0.002N\ rate - 13.14BD + 1.499pH + 2.177soil\ total\ N + 0.67N\_times + Coefficient_1 + Coefficient_2 + \varepsilon$	Maize:0; Wheat:0.845; Vegetable:-1.098 CI:0; Min:0.0020; Org:0.0006; MinOrg:-0.0016	0.80
YR (n=294)	$\ln(Cum\ NH_3) = -4.42 + 0.0067N\ rate + 0.225Temp + 0.135pH + 0.399soil\ total\ N + 0.200N\_times + Coefficient_1 + Coefficient_2 + \varepsilon$	Others:0; Rice:0.721; Vegetable:-0.532 CI:0; Min:0.0001; Org:0.0021; MinOrg:-0.0013	0.62
SSW (n=73)	$\ln(Cum\ NH_3) = 1.292 + 0.0044N\ rate - 0.019Clay - 0.0015Prec + 0.477N\_times + Coefficient_1 + Coefficient_2 + \varepsilon$	Legume:0; Rice:3.429; Others:2.295 Org:0; Min:0.0035	0.48
All-China (n=717)	$\ln(Cum\ NH_3) = -2.768 + 0.004N\ rate + 0.220pH + 0.299soil\ total\ N - 0.0006Prec + 0.225N\_times + Coefficient_1 + Coefficient_2 + \varepsilon$	Legume:0; Others:1.466; Rice:2.004; Maize:1.389; Wheat:2.178; Vegetable:0.836 CI:0; Min:0.0002; MinOrg:-0.0002; Org:0.0010	0.45

Cum NH_3 is the cumulative seasonal NH_3 emissions in kg N ha^{-1}; *N rate* represents the application amount of nitrogen fertilizer in kg N ha^{-1}; *BD* is soil bulk density in g cm^{-3}; *soil total N* is soil total nitrogen content in g kg^{-1}; *Temp* means the annual average temperature in ℃; *Prec* means the annual precipitation in mm; *N_times* means fertilization times; *Coefficient$_1$* represents the coefficients for different crop types, and *Coefficient$_2$* represents the coefficients for fertilizer type.

3.2 Model Accuracy Evaluation

According to the comparison of the model performances, the agro-region-specific models had higher R^2 (0.44) and ME (0.40) values than the national-scale model (R^2: 0.27; ME: 0.21), indicating a better fit of agro-region-specific model (Table 3). According to the agro-region-specific models, the correlation of simulated vs. measured values had R^2 values of 0.31–0.93, demonstrating a significant relationship between the simulated and measured values (Fig. 3). As shown in Table 3, the close model fit was also reflected in the positive ME values between 0.18 and 0.72. There was no significant model bias in the simulation of NH_3 emissions in LPIM, YR, HHH and SSW agro-regions, but the models underestimated the emissions by 3.38 and 3.46 kg N ha^{-1} on average in NE and GXQT agro-region.

Table 3 Statistics describing the performance of the models for cumulative NH_3 emissions simulations

Models	R^2	rRMSE (%)	ME	M (kg N ha^{-1})	t-test
National-scale (n=234)	0.27	85	0.21	3.54	s
NE (n=56)	0.18	85	0.12	2.04	ns
LPIM (n=15)	0.12	89	-0.57	8.76	s
GXQT (n=21)	0.49	93	0.31	7.84	ns
HHH (n=24)	0.24	60	-0.02	5.40	s
YR (n=88)	0.22	86	0.18	2.55	ns
SSW (n=30)	0.35	74	0.25	4.47	ns
Agro-region-specific (n=234)	0.44	74	0.40	3.30	s
NE (n=56)	0.32	76	0.25	3.38	s
LPIM (n=15)	0.63	36	0.58	1.98	ns
GXQT (n=21)	0.93	44	0.72	3.46	s
HHH (n=24)	0.45	54	0.18	2.72	ns
YR (n=88)	0.31	80	0.32	4.45	ns
SSW (n=30)	0.46	66	0.49	2.95	ns

s, significant; ns, not significant.

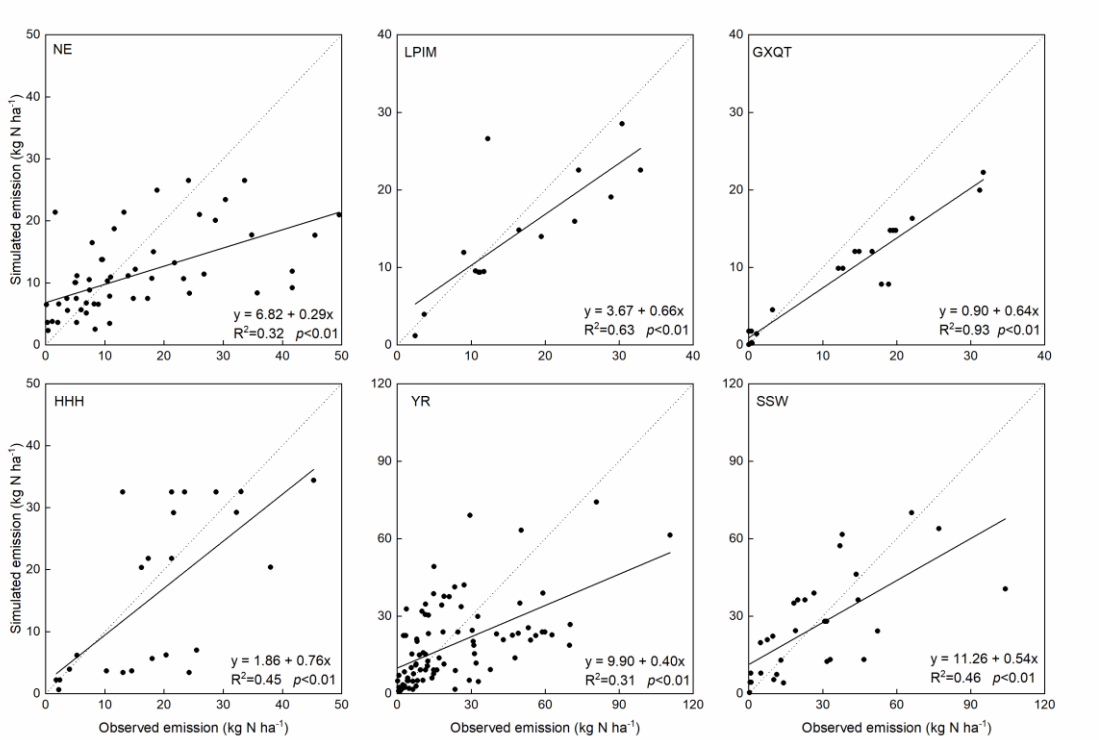

Fig. 3 Comparison of observed and simulated cumulative NH_3 emissions for six agro-regions. Solid lines represent the regression lines and dotted lines represent 1:1 (y=x) line.

3.3 NH_3 emissions of agro-regions and crop types in China

By inputting the high-spatial-resolution database into the developed models, the NH_3 emissions from China's cropland in 2015 could be mapped for each 5×5 min grid cell. The NH_3 emission intensity of different crops was first compared in different agro-regions. The average NH_3 emission intensity of cropland in China was 27.7 kg NH_3-N ha^{-1}. Grain crop cultivation had the highest emission intensity of 37.6 kg NH_3-N ha^{-1}, compared with legume cultivation with the minimum emission intensity of 4.0 kg NH_3-N ha^{-1} (Table 4). Among different grain crops, the emission intensity of rice cultivation (47.2 kg NH_3-N ha^{-1}) was higher than that of maize (26.7 kg NH_3-N ha^{-1}) and wheat (23.0 kg NH_3-N ha^{-1}) (Table S4). The highest average emission intensity of 43.2 kg NH_3-N ha^{-1} was observed in the S agro-region, while the lowest was observed for the QT agro-region, with a value of 17.2 kg NH_3-N ha^{-1} (Fig. 4A, Table 4). According to correlation analysis, the variation of emission intensity between agro-regions was related to climate conditions, fertilizer application rates and planting structure (Table S5).

Table 4 Seasonal NH_3 emission intensities in China's cropland (kg NH_3-N ha^{-1})

Region	Grain crops	Legumes	Oil-bearing crops	Vegetable	Fruit	Industrial crops	All crops
NE	17.7	4.5	5.1	6.9	19.2	3.0	18.4
YR	60.3	5.2	19.7	5.3	62.2	41.4	36.6
HHH	33.0	1.3	11.3	16.4	43.9	13.3	25.9
S	78.2	6.0	10.9	13.0	11.3	26.9	43.2
SW	38.4	2.7	5.7	14.5	16.0	3.2	27.8
GX	26.5	4.3	12.1	8.7	32.4	12.2	20.9
QT	22.6	3.9	13.1	16.5	24.0	0	17.2
IM	29.0	3.8	6.0	6.6	23.8	5.8	20.9
LP	24.1	3.9	6.2	8.0	20.6	4.3	18.6
Nationwide	37.6	4.0	12.1	11.0	26.6	17.5	27.7

The NH_3 emissions exhibited significant spatial variability, with the highest NH_3 emissions observed for the YR (1.504 Tg NH_3-N yr^{-1}) and the HHH (0.823 Tg NH_3-N yr^{-1}) agro-regions, while the emissions in the GX (0.135Tg NH_3-N yr^{-1}) and QT (0.009 Tg NH_3-N yr^{-1}) regions were relatively low (Fig. 4B, Table 5). For different crop types, the lowest NH_3 emissions of 0.043 Tg NH_3-N yr^{-1} were observed in legume cultivation, but grain crop cultivation had the highest emissions of 3.49 Tg NH_3-N yr^{-1}, accounting for 81% of the total NH_3 emissions in cropland (Table 5). In summary, the NH_3 emissions in China's cropland were estimated to be 4.31 Tg NH_3-N yr^{-1} in 2015, with a 95% CI of 3.64–5.64 Tg NH_3-N yr^{-1}. The estimation of NH_3 emissions in the GX and QT regions had the lowest uncertainty (23%) on average, and the greatest uncertainty being 91% was observed in the HHH region (Table 5).

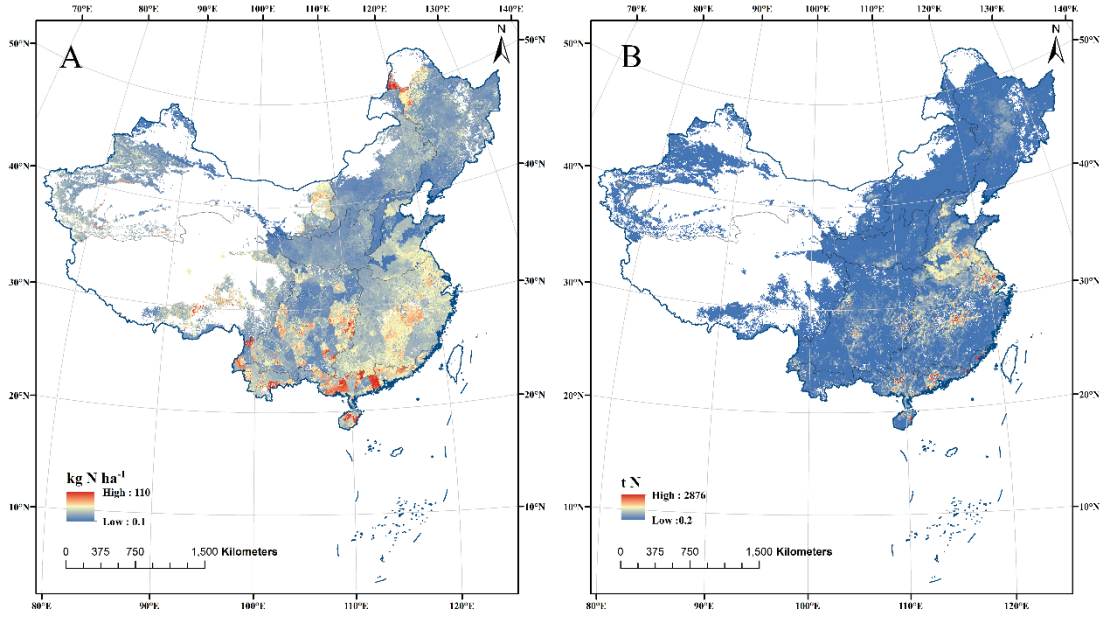

Fig. 4 Geographical distribution of NH_3 emission intensities per hectare (A) and total emissions (B) in croplands of China

Table 5 NH_3 emissions in China's cropland (Gg NH_3-N)

Region	Grain crop		Legume		Oil-bearing crop		Vegetable		Fruit		Industrial crop		All crops	
	Est.	95%CI	Est.	95%CI	Est.	95%CI	Est.	95%CI	Est.	95%CI	Est.	95%CI	Est.	95%CI
NE	367.1	257.2-536.8	17.9	13-25.2	4.1	2.9-5.7	12.6	9.1-17.8	13.6	9.9-19.2	0.5	0.4-0.8	415.7	305.6-585.8
YR	1241.5	859.1-2126.2	12.0	6.9-21.3	93.5	54-165.6	32.6	18.0-61.0	83.6	48.2-148.3	41.1	23.6-73.2	1504.4	1117.6-2395.4
HHH	672.5	219.1-1417.4	1.7	0.6-3.5	25.7	9.0-52.3	69.0	23.8-142.6	41.4	14.6-84.3	12.6	4.4-25.7	822.8	366.0-1573.1
S	369.5	220.2-690.5	2.1	1.5-4.6	7.8	3.4-17.5	36.5	17.6-77.1	30.2	13.6-67.0	24.4	11-54.2	470.5	318.4-797.6
SW	470.3	258.1-882.6	4.5	1.5-14	17.2	5.5-53.8	107.4	36.1-328.9	22.4	9.8-50.0	3.0	1.2-7.2	624.7	400.2-1095.1
GX	86.3	54.2-134.5	0.4	0.3-0.7	3.5	2.3-5.4	4.1	2.5-6.6	17.8	10.3-30.7	23.3	14.5-38.0	135.4	101.2-187.5
QT	5.0	3.1-8.0	0.5	0.3-0.8	1.6	1.1-2.4	1.4	0.8-2.3	0.1	0.1-0.4	/	/	8.6	6.6-11.8
IM	123.8	70.5-233.9	2.2	1.3-4.1	4.5	2.6-8.4	6.9	3.8-12.9	4.0	2.3-7.5	0.4	0.3-0.8	141.9	88.4-252.3
LP	150.2	75.5-306.2	2.0	1.2-3.7	3.4	2-6.3	14.3	8.1-26.6	20.2	11.7-37.6	0.4	0.2-0.7	190.6	115.1-348.0
Nationwide	3486.2	2766.9-5095.3	43.3	31.2-70.0	161.2	121.7-275.9	284.7	197.8-550.1	233.3	169.3-422.4	105.7	71.5-200.7	4314.5	3640.9-5638.8

Est.: estimated value; CI: confidence interval. The values of each crop type were seasonal emissions, and the values of "All crops" were annual emissions.

4 Discussion

4.1 Variables included in the NH_3 volatilization model

The results of this study indicate that the agro-region-specific NH_3 model performed better than the single national model (Table 3). This is mainly due to several reasons. First, most observations (60%) were obtained in the YR and NE agro-regions, and only 40% of the observations were obtained from other agro-regions; thus, the single model mainly reflected the characteristics of the YR and NE agro-regions (Fig. 1; Table S1). The single model failed to simulate the LPIM and HHH agro-regions with the negative ME values, while the simulation accuracy for the YR and NE agro-regions was also improved when the region-specific model was adopted (Table 3). Second, different agro-regions have quite different climatic and soil conditions, and the management patterns of various crop cultivation also differed, resulting in different responses of NH_3 volatilization (Table S1 and S6).

As the most important variables, N fertilization (type, rate and/or times) was included in all models and explained as high as 13–54% of the variation (Fig. 2). The marginal effect of N fertilization rate, i.e., the proportion of added N fertilizer that was ultimately volatilized as NH_3, showed obvious regional variation. For most agro-regions except the GXQT, the marginal effect was 12% on average, while the value of the GXQT was as low as 6%. This may be due to the low mean annual temperature and annual precipitation in this region, which was not conducive to the NH_3 production and volatilization (Table S6).

The responses of NH_3 volatilization to organic material application varied widely (Table 2). Organic material application induced less NH_3 volatilization than chemical fertilizer application with the same N inputs in most agro-regions, which was mainly because organic materials were generally incorporated into the soil as a base fertilizer, and organic materials released N at a slower rate than urea (Huang et al., 2016). However, organic manure application induced more NH_3 volatilization than chemical fertilizer application in YR region. Previous studies have also reported that manure application increased NH_3 volatilization, which can be related to the original nature of manure and application methods (Wang et al., 2017; Holly et al., 2017; Evans et al., 2018). The manure with low water content, high NH_4^+-N content and/or high pH had higher NH_3 volatilization, and the NH_3 volatilization under broadcast fertilization was higher than that under deep application (Paramasivam et al., 2009; Fangueiro et al., 2015; Webb et al., 2010). Inhibition

of NH_3 volatilization by inhibitors or controlled release fertilizers was also observed in most regions in this study. However, NH_3 volatilization under controlled release fertilizers (no data for inhibitors application in NE) was higher than that under typical fertilization in the NE region (Table 2). Zhang et al. (2018) found that high level controlled-release urea application resulted in a high NH_4^+-N content in the soil, which in turn emitted increased quantities of NH_3.

N fertilizer is usually applied as base fertilizer, topdressing and panicle fertilizer at different crop growth periods. The times of fertilizations greater than 1 means that the topdressing was carried out in the crop growth period. This study observed a positive response of NH_3 volatilization to the times of fertilizations in agro-regions except the NE (Table 2). This is because the method of topdressing was generally sprinkling, which can induce the N loss; on the other hand, the temperature during topdressing was higher than that of the base fertilizer application, which also led to high NH_3 volatilization.

Soil properties were presented as the other important variables in all agro-region-specific models, contributing 4%–50% of the variation (Table 2; Fig. 2). However, the soil variables included in each agro-region were different. A positive correlation between soil pH and NH_3 volatilization was observed in the models of GXQT, HHH and YR (Table 2). Soil pH determines the dynamic equilibrium of the NH_4^+-N and NH_3 in the soil; as the soil pH increases, the content of free NH_3 in the liquid phase increases, resulting in an increased potential of volatilization (Du Plessis& Kroontje, 1964). NH_3 volatilization of soil with pH > 8.5 was 61% higher than that of soil with 5.5 < pH < 7.3, and 80% higher than soil with pH ≤ 5.5 (IFA, 2001). In our dataset, the soil pH in the GXQT and HHH was higher than that in the YR (Table S6), thus the contributions of soil pH in the models of GXQT and HHH were higher than that in the YR model (Fig. 2). However, soil pH was not included in the models of NE, LPIM and SSW, which may be due to the small spatial fluctuation of soil pH, resulting in the effects of other variables masking the effects of soil pH (CVs of soil pH being 1.8%~15.1% in Table S6). Soil total N content remained in the models of LPIM, YR and HHH, indicating the role of soil N mineralization in NH_3 volatilization. The contribution of soil total N content in the LPIM model (47%) was much higher than that in the YR (9%) and HHH (1%) models (Fig. 2). Arid climates with low precipitation can increase soil N mineralization (Zhang et al., 2020), while the LPIM agro-region had the lower precipitation than the HHH and YR agro-regions.

A significant negative correlation between clay content and NH_3 volatilization was observed in the LPIM, YR and HHH regions. Soil clay has a strong adsorption effect on NH_4^+, which can effectively avoid vertical leaching of N and enrich N in topsoil (Owino et al., 2006). In addition, soils with high clay contents have poor aeration and could hinder the diffusion of NH_3 (Rawls et al., 2003; Pelster et al., 2019). Similarly, soils with high bulk density are heavy or compacted, which could increase adsorption of N and hinder the diffusion of NH_3, so there was a negative correlation between soil bulk density and NH_3 volatilization in the HHH region. However, a positive correlation was found in the NE agro-region. Zhou et al. (2016) found that the bulk density and NH_3 volatilization can have a positive correlation when the bulk density was lower than 1.4 g cm^{-3}. According to our dataset, the bulk density of NE agro-region ranged from 1.2–1.47 g cm^{-3} with an average value of 1.33 g cm^{-3}, while that of HHH agro-region was 1.3–1.6 g cm^{-3} with an average value of 1.42 g cm^{-3} (Table S6).

Climate variables were included in the models of GXQT, LPIM, YR and SSW regions with great climate variability though the relative contribution was as low as 1–12% (Table 2 and S7; Fig. 2). NH_3 volatilization was positively correlated with annual mean temperature but negatively correlated with rainfall according to this study (Table 2). High temperature can stimulate the activity of soil urease and reduce the solubility of NH_3 in soil water, which further increased NH_3 volatilization (Freney et al., 1983; Sommer et al., 1991). Infiltration of rainwater introduced N into deep soil, increasing the chance of NH_4^+-N being adsorbed by soil colloids or plant root (Nicholson et al., 2013).

This study found that NH_3 volatilization varied greatly between different crops, and paddy rice cultivation had a high NH_3 volatilization rate, but legume crop cultivation had the low one (Table 2). The paddy fields were under flooded conditions, so the applied urea can be hydrolyzed quickly and produce high pH condition (Zhao et al., 2009; Xia et al., 2010; Zhou et al., 2016). In addition, the mean air temperature in the rice growing season was high, and the high temperature and high evaporation rate could cause the NH_3 to escape with a large amount of water vapor (Li et al., 2008; Xia et al., 2010). Legumes fix atmospheric N, so the N fertilizer input was 53 kg N h^{-1} on average according to our dataset, which is lower than for other crops. Low N inputs in legume systems allowed plants and soil microbes to compete for limited available N, resulting in a low NH_3 loss (Chen et al., 2019).

4.2 Role of NH_3 emissions from China's cropland

Although the estimates for 2015 for this study are up to date, we can still compare them with estimates after 2010. The estimate of NH_3 emissions from paddy rice cultivation in 2015 (1.88 Tg N) is close to the estimate of 1.7 Tg N in 2013 using the NARSES model by Wang et al. (2018). Our estimate of national emissions (4.31 Tg NH_3-N) is close to the values of 4.3 and 4.5 Tg NH_3-N in 2010 estimated by corrected emission factor method and DLEM-Bi-NH_3 model simulation, but is significantly higher than the estimate of 3 Tg NH_3-N in 2011 by EPIC-CMAQ model (Xu et al., 2015; 2018; Fu et al., 2015). Unfortunately, none of the above-mentioned previous studies have quantified the uncertainty of the estimates, and uncertainty analysis of NH_3 emission estimation was also very limited in previous global studies (Olivier et al., 1998; Riddick et al., 2016). An uncertainty of model estimates was quantified as -15.6% (lower limit) and 30.7% (upper limit) in this study, which is much lower than the uncertainty of greater than 50% indicated by Streets et al. (2003), Zhang et al. (2011) and Huang et al. (2012), and close to the uncertainty of 19% assessed by Zhou et al. (2016) using the Bayesian Recursive Regression Tree algorithm.

A large agro-regional variation of NH_3 emission intensity was observed in this study (Table 4). A correlation analysis of various variables and emission intensity was conducted to analyze the causes of regional variation. Taking grain crops as an example, the average NH_3 emission intensities in agro-regions were significantly positively correlated with annual average temperature and annual precipitation, but slightly positively correlated with N application rate (Table S5). This indicated that the agro-regional variation of NH_3 volatilization were mainly driven by climate conditions, followed by management patterns. NH_3 volatilization was high in regions with hot and humid climates, which can promote the activity of microorganisms and urease to stimulate the hydrolysis of urea and volatilization of NH_3 (Freney et al., 1983; Sommer et al., 1991; Zhang et al., 2011). Moreover, the average emission intensities of the agro-regions with large rice planting area (NE, YR, SW, and S agro-regions) were higher than that of other regions because the emission intensity of paddy rice was higher than other crops (Table S4).

Recently, global NH_3 emissions from N fertilizer use in 2010 were estimated at 16.7 Tg NH_3-N based on DLEM-Bi-NH_3 model (Xu et al., 2019). According to this study, the emissions of China's cropland in 2015 accounted for 25.7% of the global NH_3 emissions in 2010, indicating the important role of China's NH_3 emissions globally. In addition, NH_3 emissions from China's

cropland increased from 2.8–3.7 Tg NH_3-N in 1990 to the current 4.31 Tg NH_3-N, with a growth rate of 32% on average, posing a threat to human health and environmental quality (Olivier et al., 1998; Xu et al., 2018). N fertilizer application rate and fertilizer type have an impact on NH_3 volatilization, indicating potential emission mitigation through optimizing management modes (Fig. 2). Reducing N fertilizer application is a direct means of emission mitigation. According to this study, less N fertilization of 1 kg will lower NH_3 emissions by about 0.06–0.17 kg NH_3-N ha^{-1} in different agro-regions, and further calculations showed that national emissions from paddy rice cultivation could be lowered by 14% if N fertilizer application was reduced by 10%. According to a recent meta-analysis, using non-urea fertilizers such as ammonium nitrate and ammonium sulphate could greatly reduce emissions, by 63.5% on average (Pan et al., 2016). In addition, enhanced efficiency fertilizers could also avoid NH_3 volatilization by 53.7%, which was also observed in the models of the YR and HHH agro-regions in this study (Table 2). Some amendments, such as zeolite, pyrite, organic acid and aged acidic biochar, have also been shown to be viable ways to mitigate NH_3 volatilization (Pan et al., 2016; Esfandbod et al., 2017; Sha et al., 2019).

4.3 Limitations of this study

The uncertainty range of the agro-region-specific model was acceptable for a regional NH_3 inventory, indicating that the model can be widely applied in case of limited data. However, the values R^2 were not high in the models of some regions such as the NE and SSW regions, which means that some variation was not captured by the models. Therefore, there were still some uncertainties that were not considered in this study.

Taking into account more variables can reduce uncertainty in the modeling. Wind speed is also a climate factor affecting NH_3 volatilization in farmland, and NH_3 volatilization generally increases with increasing wind speed (Sharpe et al., 1995; Wang et al., 2018). Wind speed data was rarely reported in the studies, resulting in this variable not entering the model in this study. Some previous studies made a more detailed division of fertilizer types including, for example, urea, ammonium bicarbonate, ammonium sulfate, ammonium nitrate, and diammonium phosphate, corresponding to different emission factors (Bouwman et al., 1997; Zhang et al., 2011). Unfortunately, the type of inorganic N fertilizer in our database only includes urea and ammonium

bicarbonate, and less than 10 measurements were reported under ammonium bicarbonate-only application, making model development infeasible. Fertilization methods also have an effect on NH_3 volatilization, and the incorporation of N fertilizer into the soil decreased the NH_3 volatilization compared with the surface application according to previous studies (Xia et al., 2020). The fertilization methods cannot be clearly distinguished in this study, because in general the base fertilizer was incorporated into the soil and topdressing was applied to the surface. Liquid phase pH plays an important role in NH_3 volatilization. As indicated in previous studies, and the high pH in floodwater had a promoting effect on NH_4^+ dissociation to liquid-phase NH_3 in paddy fields (Hayashi et al., 2006; 2008). However, the pH of floodwater in paddy rice growth period showed great temporal variability, and only 8 studies monitored liquid phase pH in this database (Table S1), which prevented this variable from being taken into account in the model.

The method and frequency of measurement may also induce uncertainty. Continuous airflow enclosure method (467 observations) and ventilation method (392 observations) were the main determination methods in this database, and there were also a few studies using other methods, such as the micrometeorological gradient diffusion method, wind tunnel method, and the closed-chamber method (Table S1). Different determination methods may lead to the difference of data quality, and then affect the simulation accuracy. . Crop plants also play an important role in atmosphere-cropland NH_3 exchange (Schjoerring et al., 1998). It had been confirmed that NH_3 can be emitted through crop plants, and crop plants can also recapture part of the volatile NH_3 from soil or surface water (Schjoerring et al., 1998; Hayashi et al., 2008; Katata et al., 2013). However, most studies (97%) did not include plants in monitoring, which may affect the estimation of net ammonia exchange in the whole ecosystem. This issue should be paid attention to in future studies. The measurement interval varied between 8:00-10:00 a.m. and 3:00-5:00 p.m. in the collected studies; however, Cao et al. (2013) indicated that NH_3 fluxes based on the dynamic chamber method measured at 10:00-11:00 a.m. or 4:00-5:00p.m. intervals could lead to large inherent variability of NH_3 fluxes.

5 Conclusion

Based on the establishment of a database, single national and agro-region-specific NH_3 volatilization models were both developed using stepwise regression methods. The performance of the agro-region-specific models was better than that of the single national model. Significant contributions of climate, soil and management variables were observed in the developed models. The total amount of NH_3 emissions induced by chemical N fertilizer input in China's cropland was calculated to be 4.31 Tg NH_3-N in 2015, with a 95% CI of 3.64−5.64 Tg NH_3-N yr^{-1}, to which paddy rice cultivation made the greatest contribution.

ACKNOWLEDGMENTS

This work was financially supported by Natural Science Foundation of China under a grant numbers 41877546 and U1612441, and a BBSRC-Newton Funded project (BB/N013484/1). This work also contributes to the activities of Top-notch Academic Programs Project of Jiangsu Higher Education Institution of China (PPZY2015A061), and Program for Student Innovation through Research and Training (1913A22).

ASSOCIATED CONTENT

Supporting Information

Supplementary results of model information, supplementary results of NH_3 emissions, detailed data information about variables entering the models (PDF)

Database (XLSX)

References

Anderson N, Strader R, Davidson C. Airborne reduced nitrogen: ammonia emissions from agriculture and other sources. *Environment International*, **2003**, *29(2-3)*: 277-286.

Battye, W.; Aneja, V. P.; Roelle, P. A.Evaluation and improvement of ammonia emissions inventories. *Atmospheric Environment*, **2003**, *37(27)*: 3873-3883.

Bouwman, A. F.; Lee, D. S.; Asman, W. A. H.; Dentener, F. J.; Van Der Hoek, K. W.; Olivier, J. G. J. A global high-resolution emission inventory for ammonia. *Global Biogeochemical Cycles*, **1997**, *11(4)*: 561-587.

Bouwman, L. Global assessment of acidification and eutrophication of natural ecosystems. *UNEP/Earthprint*, **1999**.

Cao, Y.; Tian, Y.; Yin, B.; Zhu, Z. Assessment of ammonia volatilization from paddy fields under crop management practices aimed to increase grain yield and N efficiency. *Field Crops Research*, **2013**, *147*: 23-31.

Chambers, J. M.; Hastie T. J. Statistical Models in S// Statistical models in S. Wadsworth & Brooks/Cole. 1993.

Chen, P.; Song, C.; Liu, X.; Zhou, L.; Yang, H.; Zhang, X.; Zhou, Y.; Du, Q.; Pang, T.; Fu, Z.; Wang, X. Yield advantage and nitrogen fate in an additive maize-soybean relay intercropping system. *Science of the Total Environment*, **2019**, *657*, 987-999.

Department of Price in National Development and Reform Commission of China (DP-NDRC). Compilation of the National Agricultural Costs and Returns; China Statistics Press, Beijing, 2016.

Department of Rural Social Economical Survey, State Bureau of Statistics (DRSES-SBS). China Rural Statistical Yearbook. China Statistics Press, Beijing, China, 2016.

Du Plessis, M. C. F., & Kroontje, W. (1964). The relationship between pH and ammonia equilibria in soil. Soil Science Society of America Journal, 28(6), 751-754.

Esfandbod, M.; Phillips, I. R.; Miller, B.; Rashti, M. R.; Lan, Z. M.; Srivastava, P.; Singh, B.; Chen, C. R. Aged acidic biochar increases nitrogen retention and decreases ammonia volatilization in alkaline bauxite residue sand. *Ecological Engineering*, **2017**, *98*, 157-165.

Evans, L.; VanderZaag, A. C.; Sokolov, V.; Baldé, H.; MacDonald, D.; ClaudiaWagner-Riddle.; Gordon, R. Ammonia emissions from the field application of liquid dairy manure after

anaerobic digestion or mechanical separation in Ontario, Canada. *Agricultural and Forest Meteorology*, **2018**, *258*: 89-95.

Fangueiro, D., Hjorth, M., & Gioelli, F. (2015). Acidification of animal slurry– a review. Journal of Environmental Management, 149, 46–56. https://doi.org/10.1016/j.jenvman.2014.10.001

FAO (**2018**) FAOSTAT *Emissions Database*, *Agriculture*, *Agriculture Total*, http://www.fao.org/faostat/en/#data/GT (accessed October 22, 2019)

FAO/IIASA/ISRIC/ISS-CAS/JRC. Harmonized World Soil Database (Version 1.2). FAO, Rome, Italy and IIASA, Laxenburg, Austria, 2012

Freney, J. R.; Simpson, J. R. Gaseous loss of nitrogen from plant-soil systems. *Springer Science & Business Media*, **1983**.

Fu, X.; Wang, S.; Ran, L. M; Pleim, J. E.; Cooter, E.; Bash, J. O.; Benson, V.; Hao, J. M. Estimating NH_3 emissions from agricultural fertilizer application in China using the bi-directional CMAQ model coupled to an agro-ecosystem model. *Atmospheric Chemistry and Physics*, ***2015***, *15(12)*: 6637-6649.

Galloway, J. N.; Dentener, F. J.; Capone, D. G.; Boyer, E. W.; Howarth, R. W.; Seitzinger, S. P.; Asner, G. P.; Cleveland, C. C.; Green, P. A.; Holland, E. A.; Karl, D. M.; Michaels, A. F.; Porter, J. H.; Townsend, A. R.; Vöosmarty, C. J. Nitrogen cycles: past, present, and future. *Biogeochemistry*, **2004**, *70(2)*: 153-226.

Gao, Z.; Ma, W.; Zhu, G.; Ma, W.; Roelcke, M. Estimating farm-gate ammonia emissions from major animal production systems in China. *Atmospheric Environment*, **2013**, *79*: 20-28.

Hayashi, K., Nishimura, S., & Yagi, K. (2006). Ammonia volatilization from the surface of a Japanese paddy field during rice cultivation. Soil Science and Plant Nutrition, 52(4), 545–555.

Hayashi, K., Nishimura, S., & Yagi, K. (2008). Ammonia volatilization from a paddy field following applications of urea: Rice plants are both an absorber and an emitter for atmospheric ammonia. Science of The Total Environment, 390(2), 485–494.

Holly, M. A.; Larson, R. A.; Powell, J. M.; Ruark, M. D.; Aguirre-Villegas, H. Greenhouse gas and ammonia emissions from digested and separated dairy manure during storage and after land application. Agriculture, Ecosystems & Environment, 2017, 239: 410-419.

Huang, S., Lv, W., Bloszies, S., Shi, Q., Pan, X., & Zeng, Y. (2016). Effects of fertilizer

management practices on yield-scaled ammonia emissions from croplands in China: a meta-analysis. Field crops research, 192, 118-125.

Huang, X.; Song, Y.; Li, M.; Li, j.; Huo, Q.; Cai, X.; Zhu, T.; Hu, M.; Zhang, H. A high-resolution ammonia emission inventory in China. *Global Biogeochemical Cycles*, **2012**, *26*(1).

Intergovernmental Panel on Climate Change (IPCC). 2019. Chapter 5: cropland land. In: Blain, D., Agus, F., Alfaro, M.A., Vreuls, H. (Eds.), 2019 Refinement to the 2006 IPCC Guidelines for National Greenhouse Gas Inventories, vol. 5. Agriculture, Forestry and Other Land Use, p. 68. IPCC (advance version).

Intergovernmental Panel on Climate Change (IPCC). 2000. IPCC Good Practice Guidance and Uncertainty Management in National Greenhouse Gas Inventories. Hayama, Japan.

International Fertilizer Association (IFA). Global estimates of gaseous emissions of NH_3, NO and N_2O from agricultural land. Food and Agriculture Organization of the United Nations (FAO), 2001.

Katata, G., Hayashi, K., Ono, K., Nagai, H., Miyata, A., & Mano, M. (2013). Coupling atmospheric ammonia exchange process over a rice paddy field with a multi-layer atmosphere–soil–vegetation model. Agricultural and Forest Meteorology, 180, 1–21.

Krupa, S. V. Effects of atmospheric ammonia (NH_3) on terrestrial vegetation: a review. *Environmental Pollution*, **2003**, *124(2)*: 179-221.

Li, H.; Liang, X.; Chen, Y.; Tian, G.; Zhang, Z. Ammonia volatilization from urea in rice fields with zero-drainage water management. *Agricultural Water Management*, **2008**, *95(8)*, 887-894.

Monfreda, C.; Ramankutty, N.; Foley, J. A. Farming the planet: 2. Geographic distribution of crop areas, yields, physiological types, and net primary production in the year 2000. *Global Biogeochemical Cycles*, **2008**, *22(1)*; DOI: 10.1029/2007GB002947.

Mueller, N. D.; Gerber, J. S.; Johnston, M.; Deepak, K.; Ramankutty, N.; Foley, J. A. Closing yield gaps through nutrient and water management. *Nature*, **2012**, *490(7419)*: 254.

National Agricultural Regionalization Committee (NARC). Comprehensive Agricultural Regionalization in China. Beijing: China Agriculture Press, 1991.

Nicholson, F. A.; Bhogal, A.; Chadwick, D. E. Gill.;Gooday, R. D.; Lord, E.; Misselbrook, T.; Rollett, A. J.; Sagoo, E.; Smith, K. A.; Thorman, R. E.; Williams, J. R.; Chambers, B. J. An

enhanced software tool to support better use of manure nutrients: MANNER-NPK. *Soil Use and Management*, **2013**, *29(4)*: 473-484.

Olivier, J. G. J.; Bouwman, A. F.; Van der Hoek, K. W.; Berdowski, J. J. M. Global air emission inventories for anthropogenic sources of NOx, NH_3 and N_2O in **1990**. *Environmental Pollution*, **1998**, *102(1)*: 135-148.

Owino, J. O.; Owido, S. F. O.; Chemelil M, C.; Nutrients in runoff from a clay loam soil protected by narrow grass strips. *Soil and Tillage Research*, **2006**, *88(1-2)*: 116-122.

Pan, B.; Lam, S.; Mosier, A.; Luo, Y.; Chen, D. Ammonia volatilization from synthetic fertilizers and its mitigation strategies: a global synthesis. *Agriculture, Ecosystems & Environment*, **2016,** *232*: 283-289.

Paramasivam, S., Jayaraman, K., Wilson, T. C., Alva, A. K., Kelson, L., & Jones, L. B. (2009). Ammonia volatilization loss from surface applied livestock manure. Journal of Environmental Science and Health, Part B, 44(3), 317–324.

Pelster, D. E.; Watt, D.; Strachan, I. B.; Rochette, P.; Bertrand, N.; Chantigny, M. H. Effects of Initial Soil Moisture, Clod Size, and Clay Content on Ammonia Volatilization after Subsurface Band Application of Urea. *Journal of Environmental Quality*, **2019**, *48*(3), 549-558.

Rawls, W. J.; Pachepsky, Y. A.; Ritchie, J. C.; Sobecki, T. M.; Bloodworth, H. Effect of soil organic carbon on soil water retention. Geoderma **2003**, *116 (1)*, 61−76.

Riddick, S.; Ward, D.; Hess, P.; Mahowald, N.; Massad, R.; Holland, E. A. Estimate of changes in agricultural terrestrial nitrogen pathways and ammonia emissions from **1850** to present in the Community Earth System Model. *Biogeosciences*, **2016**, *13(11)*: 3397.

Schjoerring, J. K., Husted, S., & Mattsson, M. (1998). Physiological parameters controlling plant–atmosphere ammonia exchange. Atmospheric Environment, 32(3), 491–498.

Sha, Z.; Li, Q.; Lv, T.; Misselbrook, T.; Liu, X. Response of ammonia volatilization to biochar addition: A meta-analysis. *Science of the Total Environment*, **2019**, *655*, 1387-1396.

Sharpe, R. R.; Harper, L. A. Soil, plant and atmospheric conditions as they relate to ammonia volatilization//Nitrogen Economy in Tropical Soils. Springer, Dordrecht, **1995**: 149-158.

Smith, P.; Smith, J. U.; Powlson, D. S.; McGill, W. B.; Arah, J. R. M.; Chertov, O. G.; Coleman, K.; Franko, U.; Frolking, S.; Jenkinson, D. S.; Jensen, L. S.; Kelly, R. H.; Klein-Gunnewiek,

H.; Komarov, A. S.; Li, C.; JMolina, J. A. E.; Mueller, T.; Parton, J. W.; Whitmore, A. P. A comparison of the performance of nine soil organic matter models using datasets from seven long-term experiments. *Geoderma*, **1997**, *81(1-2)*: 153-225.

Sommer, S. G.; Olesen, J. E.; Christensen, B. T. Effects of temperature, wind speed and air humidity on ammonia volatilization from surface applied cattle slurry. *The Journal of Agricultural Science*, **1991**, *117(1)*: 91-100.

Streets, D. G.; Bond, T. C.; Carmichael, G. R.; Streets, D. G.; Bond, T. C.; Carmichael, G. R,; Fernandes, S. D.; Fu, Q.; He, D.; Klimont, Z.; Nelson, S. M.; Tsai, N. Y.; Wang, M.; Woo, J-H.; Yarber, K. F. An inventory of gaseous and primary aerosol emissions in Asia in the year 2000. *Journal of Geophysical Research: Atmospheres*, **2003**, *108*(D21), DOI: 10.1029/2002JD003093.

Tian, H.; Chen, G.; Lu, C.; Xu, X.; Ren, W.; Zhang, B.; Banger, K.; Tao, B.; Pan, S.; Liu, M.; Zhang, C.; Bruhwiler, L.; Wofsy, S. Global methane and nitrous oxide emissions from terrestrial ecosystems due to multiple environmental changes. *Ecosystem Health and Sustainability*, **2015**, *1(1)*: 1-20.

Wang, C.; Yin, S.; Bai, L.; Zhang, X.; Gu, X.; Zhang, H.; Lu, Q.; Zhang, R. High-resolution ammonia emission inventories with comprehensive analysis and evaluation in Henan, China, **2006–2016**. *Atmospheric Environment*, **2018**, *193*: 11-23.

Wang, Y.; Dong, H.; Zhu, Z.; Pierre, J .Gerber.; Xin, H.; Smith, P.; Opio, C.; Steinfeld, H.; Chadwick, D. Mitigating greenhouse gas and ammonia emissions from swine manure management: a system analysis. Environmental Science & Technology, 2017, 51(8): 4503-4511.

Webb, J., Pain, B., Bittman, S., & Morgan, J. (2010). The impacts of manure application methods on emissions of ammonia, nitrous oxide and on crop response—A review. Agriculture, Ecosystems & Environment, 137(1), 39–46.

Wu, S.; Zhang, Y.; Schwab, J. J.; Li, Y.; Liu, Y.; Yuan, C. High-resolution ammonia emissions inventories in Fujian, China, 2009–2015. *Atmospheric Environment*, **2017**, *162*: 100-114.

Xia, L.; Lam, S.;Yan, X.; Chen, D. How does recycling of livestock manure in agroecosystems affect crop productivity, reactive nitrogen losses, and soil carbon balance? *Environmental Science & Technology*, **2017**, *51(13)*: 7450-7457.

620 Xia, L., Li, X., Ma, Q., Lam, S. K., Wolf, B., Kiese, R., ... & Yan, X. (2020). Simultaneous
621 quantification of N2, NH3 and N2O emissions from a flooded paddy field under different N
622 fertilization regimes. Global Change Biology, 26(4), 2292-2303.
623 Xia, W.; Zhou, W.; Liang, G.; Wang, X.; Sun, J.; Li, S; Hu, C.; Chen, Y. Effect of optimized
624 nitrogen application on ammonia volatilization from paddy field under wheat-rice rotation
625 system. *Plant Nutrition and Fertilizer Science*, **2010**, *16(1)*, 6-13.
626 Xu, P.; Zhang, Y.; Gong, W.; Hou, X.; Kroeze, C.; Gao, L.; Luan, S. An inventory of the emission
627 of ammonia from agricultural fertilizer application in China for 2010 and its high-resolution
628 spatial distribution. *Atmospheric Environment*, **2015**, *115*: 141-148.
629 Xu, R.; Pan, S.; Chen, J.; Chen, G.; Yang, J.; S. R. S, Dangal.; J. P, Shepard.; Tian, H. Half-century
630 ammonia emissions from agricultural systems in Southern Asia: Magnitude, spatiotemporal
631 patterns, and implications for human health. *GeoHealth*, **2018**, *2(1)*: 40-53.
632 Xu, R.; Tian, H.; Pan, S.; Stephen, A. Prior.; Feng, Y.; William, D. Batchelor.; Chen, J.; Yang, J.
633 Global ammonia emissions from synthetic nitrogen fertilizer applications in agricultural
634 systems: Empirical and process-based estimates and uncertainty. *Global Change Biology*,
635 **2019**, *25(1)*: 314-326.
636 Yan, X.; Akimoto, H.; Ohara, T. Estimation of nitrous oxide, nitric oxide and ammonia emissions
637 from croplands in East, Southeast and South Asia. *Global Change Biology*, **2003**, *9(7)*:
638 1080-1096.
639 Yan, X.; Ti, C.; Vitousek, P.; Chen, D.; Leip, A.; Cai, Z.; Zhu, Z. Fertilizer nitrogen recovery
640 efficiencies in crop production systems of China with and without consideration of the
641 residual effect of nitrogen. *Environmental Research Letters.* **2014**, *9(9)*, 095002, DOI:
642 10.1088/1748-9326/9/9/095002.
643 Zhang, F.; Cui, Z.; Wang, J.; Li, C.; Chen, X. Current status of soil and plant nutrient management
644 in China and improvement strategies. *Chinese Bulletin of Botany*, **2007**, 24(6): 687-694. (in
645 Chinese with English summary)
646 Zhang, S.; Shen, T.; Yang, Y.; Li, Y.; Wan, Y.; Zhang, M.; Tang, Y.; Allen, S. C. Controlled-release
647 urea reduced nitrogen leaching and improved nitrogen use efficiency and yield of
648 direct-seeded rice. *Journal of Environmental Management*, **2018**, *220*: 191-197.
649 Zhang, X. Y., Li, Q. W., Gao, J. Q., Hu, Y. H., Song, M. H., & Yue, Y. (2020). Effects of rainfall

amount and frequency on soil nitrogen mineralization in Zoigê alpine wetland. European Journal of Soil Biology, 97, 103170.

Zhang, Y.; Luan, S.; Chen, L.; Shao, M. Estimating the volatilization of ammonia from synthetic nitrogenous fertilizers used in China. *Journal of Environmental Management*, **2011**, *92(3)*: 480-493.

Zhao, X.; Xie, Y.; Xiong, Z.; Yan, X.; Xing, G.; Zhu, Z. Nitrogen fate and environmental consequence in paddy soil under rice-wheat rotation in the Taihu lake region, China. *Plant and Soil*, **2009**, *319(1-2)*, 225-234.

Zhou, F.; Ciais P, Hayashi, K.; Galloway, J.; Dong-Gill Kim.; Yang, C.; Li, S.; Liu, B.; Shang, Z.; Gao, S. Re-estimating NH_3 emissions from Chinese cropland by a new nonlinear model. *Environmental Science & Technology*, **2016**, *50(2)*: 564-572.

Zuur, A.F.; Ieno, E.N.; Smith,G.M.; Analyzing Ecological Data. *Springer Science & Business Media*., **2007**.

663 Figure captions

664 Fig. 1 Geographical distribution of experimental sites in China that were used for establishment of
665 the NH_3 emission model

666 Fig. 2 Contributions of each variable to the NH_3 volatilization models

667 Fig. 3 Comparison of observed and simulated cumulative NH_3 emissions for six agro-regions.
668 Solid lines represent the regression lines and dotted lines represent 1:1 (y=x) line

669 Fig. 4 Geographical distribution of NH_3 intensities per hectare (A) and total emissions (B) in
670 croplands of China